International Journal of Computer Sciences and Engineering
Vol.**11**, Issue.**12**, pp.**01-08**, December **2023**
ISSN: 2347-2693 (Online)
Available online at: www.ijcseonline.org

ISSN: 2347-2693 (E)

Research Paper

Modeling and Simulation of LSPMSM for Estimation of Thermal Effect during Different Load Condition

Mousumi Jana Bala[1*], Chandan Jana[2], Suparna Kar Chowdhury[3], Arindam Kumar Sil[4]

[1]Department of Electrical Engineering, Meghnad Saha Institute of Technology, Kolkata, India
[2]Department of Electrical Engineering, Hooghly Engineering and Technology College, Hooghly, India
[3,4]Department of Electrical Engineering, Jadavpur University, Kolkata, India

**Corresponding Author: mousumibala@rediffmail.com*

Received: 03/Nov/2023; **Accepted**: 06/Dec/2023; **Published**: 31/Dec/2023. **DOI**: https://doi.org/10.26438/ijcse/v11i12.18

Abstract: In this work a methodology to estimate the effect of elevated temperature on a Line Start Permanent Magnet Synchronous Motor (LSPMSM) has been proposed. A simulated model of LSPMSM has been developed for Finite Element Analysis (FEA). The losses obtained from FEA were fed to a Lumped Parameter Thermal Network (LPTN) developed for LSPMSM in the LTSpice environment. The extent of demagnetisation was estimated and the FEA was conducted to identify the change in motor performance. The thermal modeling of the motor has been developed to evaluate the increase in temperature at different parts of LSPMSM under three different load conditions and even after switching off the motor. The results so obtained were validated on a physical setup. The results were analysed to ascertain the performance of the permanent magnets in LSPMSM.

Keywords: Electromagnetic Analysis, LSPMSM, Lumped Parameter Thermal Network, Thermal Analysis, Demagnetisation

1. Introduction

LSPMSMs are being extensively used in sustainable energy applications for its high torque ratio, power ratio, inherent starting torque and improved power factor. High temperature may damage the conductors, insulating materials and the permanent magnets (PMs). LSPMSMs are commonly suffered from demagnetisation of PM caused due to the rise of temperature. The maximum winding temperature of a 30.8 W, 24V PM dc Maxon motor may rise up to 155°C while its normal operating temperature is 25°C [1] and [2]. This high temperature buildup changes the PM magnetic characteristics. Performance degradation of PMSMs in terms of running torque reduction, increased losses and reversible as well as irreversible demagnetization due to high temperature has been dealt with in [3]. S.K. Chowdhury et.al developed lumped parameter thermal network (LPTN) to obtain thermal characteristics of a Totally Enclosed, Fan-Cooled (TEFC) single phase induction motor at transient condition [4]. A hybrid hydraulic-thermal bi-directional network was proposed to obtain the fluid – thermal characteristics of LSPMSM although CFD takes more time to calculate the heat coefficientS [5]. LPTN is more effective and accurate, compare to CFD for estimation of final temperature of PMSM [6, 7]. A comparative study of evaporative cooling and jacket cooling of PMSM through CFD and LPTN were proposed [8, 9]. PMSM thermal behaviors have also been obtained by Finite Element analysis [10, 11]. LPTN and 2D analytical thermal model helps to develop a hybrid lumped parameter thermal model to obtain the temperature field [12]. A lumped parameter magnetic circuit along with thermal model using current harmonics was developed for parameter estimation [13]. A thermal model which could be used with the help of interpolation to obtain the temperature rise and temperature difference of any part of PMSM for any load conditions [14]. A coupled lumped parameter magnetic circuit (LPMC) and LPTN model was proposed to calculate the electric parameters with less computational time [15]. Few authors proposed a hybrid method for estimation of temperature distribution of permanent magnets for interior type PMSM [16]. Till date most of the studies were conducted on PMSM and hence a deficiency in detailed thermal analysis on LSPMSM is realized. A study on the change in efficiency due to temperature change has been reported [17]. A software based thermal analysis of LSPMSM to obtain maximum output from a particular frame of induction motor has been presented in [18].

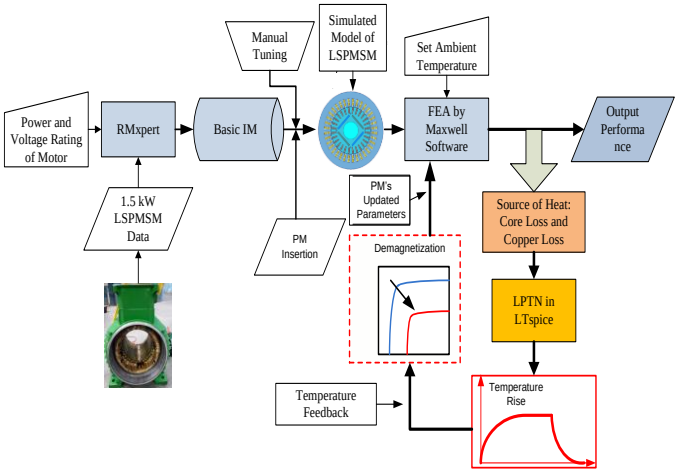

Figure 1. Flow chart for the complete methodology

While compare with induction motor it has been noticed that LSPMSM can deliver more power at a higher efficiency although the change in motor performances due to temperature variation was not considered. Condition monitoring due to thermal overloading of electric motor is discussed in several literatures which implies the importance of the thermal modeling of LSPMSM [19]. Multi-phase PMSM drive by tuning PI controller have been attained significance importance [20].

In present work, a compact modeling and design methodology has been proposed to estimate the change in the performances of LSPMSM due to the temperature rise. At first a simulated model of LSPMSM was developed by inserting the permanent magnet into the rotor of an Induction motor [21]. A simple LPTN has been developed for quick evaluation of maximum temperature of assorted parts of LSPMSM. Effect of high temperature on remanence flux density (B_r) and coercivity (H_c) of PM have been evaluated and consequently the change in performances of the LSPMSM has been estimated. As LSPMSM has both conducting bars and PMs in rotor structure, it is crucial to consider the rotor core above and below the PM and in the interpolar region separately during thermal modeling. Resistances and capacitances of thermal Equivalent circuit of LSPMSM have been calculated using various dimensional parameters. FEA has been conducted to obtain the losses, efficiency, and torque. The estimated eddy current losses of PM, core losses and copper losses were fed to the developed LPTN to obtain the temperature rise. The Driving End (DE) and Non-Driving End (NDE) thermal resistances have been carefully modeled to estimate change in temperature under different load conditions and even after switching off the motor. Effect of the PM demagnetization, on motor performances was evaluated at this elevated temperature. An experimental study was conducted on a 1.5kW LSPMSM (Synchrovert) to validate the LPTN.

2. Methodology

The whole methodology starting from designing the main dimensions from rated parameters to the estimation of the impact of elevated temperature on the motor performance includes

• Designing the motor from rated parameter
• Developing simulated model of LSPMSM in Maxwell and analyzing the design for steady state performances at normal operating temperature
• Modeling the Lumped Parameter Thermal Network (LPTN) to obtain the ultimate rise of temperature
• Estimating the consequences of demagnetization of permanent magnet on the motor performance.

The flow chart shown in Figure 1 resembles the whole process of the proposed work.

Basic induction motor frame is used to develop the simulated model of LSPMSM. The electromagnetic analysis was conducted to obtain the rated performance and the losses at ambient temperature. These losses mainly core and ohmic losses of were fed as the sources in the LPTN for thermal analysis at three different load condition. The maximum temperature rise of the PM was obtained from the thermal analysis. The degree of demagnetisation of the PM due to this increased temperature has been obtained and the degradation of the motor performances due to this was then analysed.

2.1 Dimension Design of LSPMSM

The dimensions of a 3-phase, 4 pole, 1.5 kW LSPMSM were calculated following the conventional design procedures and were then validated with the actual dimensions of the motor. The motor was designed for 112M frame and IE4 efficiency class. The core material used for stator and rotor is M235_35A. The thickness is selected as 0.35 mm for a lower value of specific core loss about 2.25 W/kg at 1.5T. N33UH which is a member of rare earth permanent magnet material NdFeB family, has been used as its remanence flux density and coercivity lie between 1.140 to 1.170 T and 830-880 kA/m respectively at 20°C. The maximum operating temperature of N33UH is 180°C. Copper and Aluminum are respectively used for stator winding ad rotor bars material. The design sheet was prepared from which losses for various parts of the motor were obtained to feed the LPTN. The results thus obtained were mentioned in the result section. The design specifications are mentioned in Table 1.

2.2 Simulated Model Development and Analysis

With the dimension obtained, a basic induction motor model has been developed in RMxpert. Now, the PM bar with the appropriate dimension and material has been inserted within the rotor. However, presence of PM in the rotor produces a negative cogging torque; sufficient value of rotor cage torque must be developed for smooth starting. The rotor bar torque vanishes, as the rotor attains the synchronous speed, the running torque being produced by the PM. Although, PM raises the overall cost of the machine, the high torque and power density of LSPMSM also could be possible as the rotor has embedded PM. As the use of PM, avoids the field winding losses, IE4 and IE5 efficiency levels could be attained for LSPMSM [22]. The shape and position of the PM in rotor structure highly influences the performance of the machine [23].

The model has been finalized through manual tuning to obtain the actual motor performance. A flux barrier of 2 mm has been inserted between two adjacent PM poles to avoid the short circuiting fluxes [24] for enhancement of the motor performances.

The FEA on dq− axis model of the developed LSPMSM has been conducted in Ansys Maxwell environment with proper grade of core and magnet material for calculating the motor performances [25].

Table 1. Specification and Dimension of LSPMSM Parameters

Parameters	Value
Power, HP	2
Voltage, volts	415
Line Current, amps	2.75
Speed, rpm	1500
Efficiency, %	89.2
Power factor	0.86
Frame size	112M
Stator ID/OD, mm	102/165
Stator Core length, mm	110
Rotor ID/OD, mm	37.2 /100.7
Rotor core length, mm	120
Slots stator/rotor	36/24
PM thickness/width, mm	3.4/40
Material Core/ PM	M235_35A/N33UH

The cross sectional view of the LSPMSM model simulated in Ansys Maxwell environment, the view of stator and permanent magnet rotor of LSPMSM used for experimental validation, are represented in Figure 2 (a), (b) and (c) respectively. Bar type PM inset rotor has been used for LSPMSM. The PM, flux barrier and rotor cage bars are showing in Figure 2 (c).

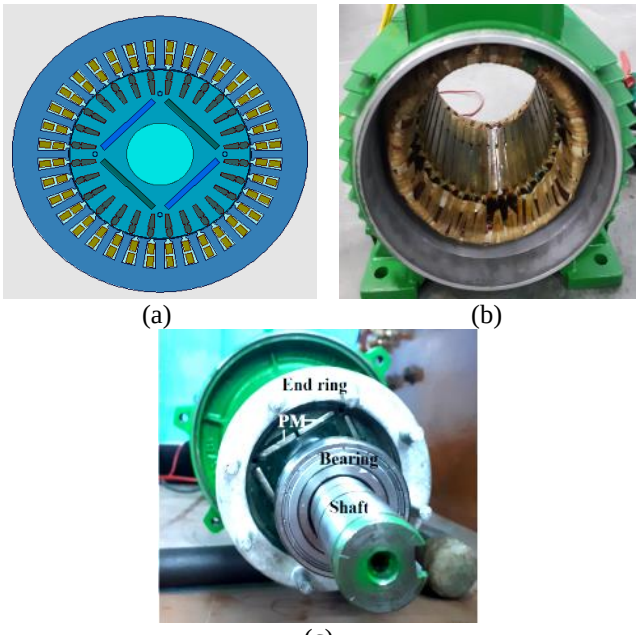

(a) (b)

(c)

Figure 2.(a) FEA model (b) Stator and (c) PM rotor of the test machine of 1.5 kW LSPMSM

2.3 Thermal Network Modeling

Thermal modeling of LSPMSM is essential at early design stage as the magnets present in the rotor could be subjected to the reversible demagnetization at an elevated temperature or could be permanently demagnetized if operating point is below the knee point on demagnetisation characteristics due to the high value of temperature rise along with an applied reversed magnetic field –H [26]. The insulation of the stator coil also could be damaged if the operating temperature is too high. A LPTN has been developed to achieve the temperature of all parts of LSPMSM during different load condition.

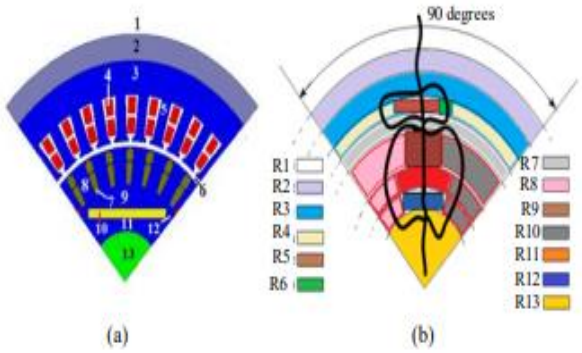

Figure 3.(a) Nodes on the LSPMSM **(b)** Corresponding resistances at the defined nodes

Each part of the motor has been represented by resistances and capacitances considering the associated process and the direction of heat flow. Among the three basic directions of heat flow, radial and axial flows have been considered as the circumferential heat flow is negligible. Due to symmetrical structure, only one fourth of its cross section is enough for thermal analysis of four pole motor. All teeth, conductors in slots, stacked liners and bars in stator and rotor are considered as lumped as shown in Figure 3 (a) and (b). The radial thermal circuit has been modeled by connecting the calculated radial thermal resistances in accordance with the heat flow path as shown by black lines in Figure 3 (b). With the PM in between shaft and the rotor bar, the rotor core has been divided into three different parts for obtaining accurate estimation of temperature. All significant parts have been represented by the thermal resistances at different nodes between 1 to13. They are mentioned below.

1	Ambient	8	Rotor teeth
2	Frame	9	Rotor core (between PM and rotor bar)
3	Stator core	10	Permanent Magnet (PM)
4	Stator teeth	11	Rotor core 1(rotor core between shaft and the PM)
5	Stator slot with conductors	12	Rotor core3 (interpolar region)
6	Air Gap	13	Shaft
7	Rotor slot		

Losses at each part of the motor have been represented by current sources at the corresponding nodes [27, 28]. Fixed magnitude voltage sources have been connected to the nodes representing the surfaces exposed to ambient.

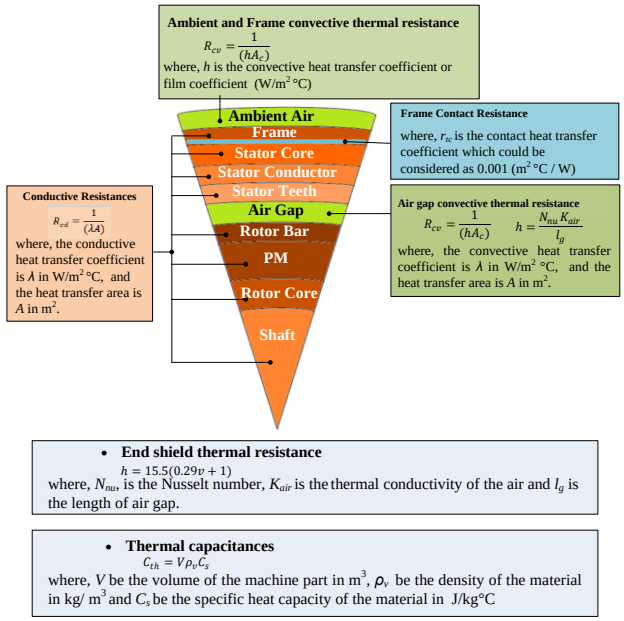

Figure 4. Calculation of different thermal resistances

Capacitances and resistances of the equivalent thermal circuit of LSPMSM have been calculated as per the formulae given Figure 4. The Nusselt number, N_{nu} while calculating the air gap film coefficient, h has been considered as mentioned in [29] and [30]. Suitable value has been selected while choosing the cooling fan efficiency at the time of calculating end shield thermal resistances [31]. Cooling fan stops to rotate after the motor is switched off. The cooling air velocity, v becomes zero which changes the magnitudes of heat transfer coefficient, h. The heat stored inside the motor dissipates slowly due to the absence of moving air and hence the slope of the cooling curves changes. The magnitudes of capacitances and resistance of the thermal equivalent circuit at NDE have been modeled accordingly. The new value of the thermal resistance has been incorporated into the model through two controlled switches sw1 and sw2 as represented in Figure 5. Thermal resistances along axial heat flow direction are calculated in between end shields at DE and NDE. In Figure 5, resistances R_1 to R_{15} and R_{36} to R_{41} represent the radial resistances whereas R_{16} to R_{35} and R_{42} to R_{43} represent the axial thermal resistances

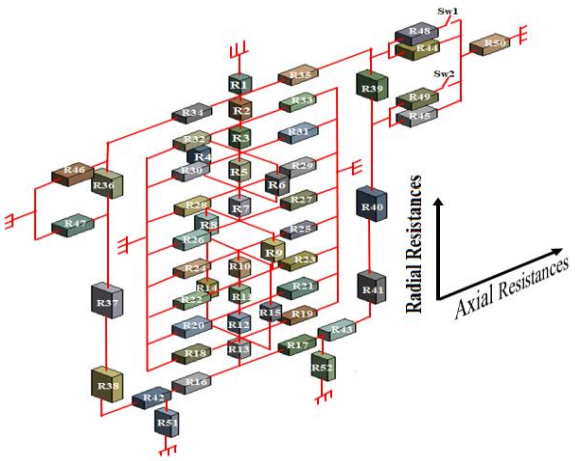

Figure 5. LPTN for LSPMSM

2.4 Effect of Temperature Rise on Motor Performance

Demagnetization of the PM results in the reduction of its remanence flux density (B_r) and coercivity (H_c). N33UH, the used PM has been modified as the following equations

$$B_{r,T} = B_{r,0}\left[1+\alpha(T-T_0)\right] \quad (1)$$

$$H_{c,T} = H_{c,0}\left[1+\beta(T-T_0)\right] \quad (2)$$

where, α is - 0.011% / ^{0}C and β is -0.06% / ^{0}C.
The high temperature of the PM caused the reduction in the flux linkage of N33UH and as the developed electromagnetic torque is a function of the pm flux linkages, there will be a reduction in the electromagnetic torque [32]. With the revised value of the PM parameters, the FEA at full load has been conducted on the developed simulated model.

3. Experimental Setup for Validation

Test has been conducted on a 1.5 kW, 415 V LSPMSM at no, half and full load condition for constant two hours and readings were taken at DE and NDE in an interval of 10 minutes using an Infrared Thermometer FT3700-20. When the motor was turned off, readings were noted frequently (after every 1min interval) for approximately 10 minutes to identify the nature of temperature rise immediately after shut down.

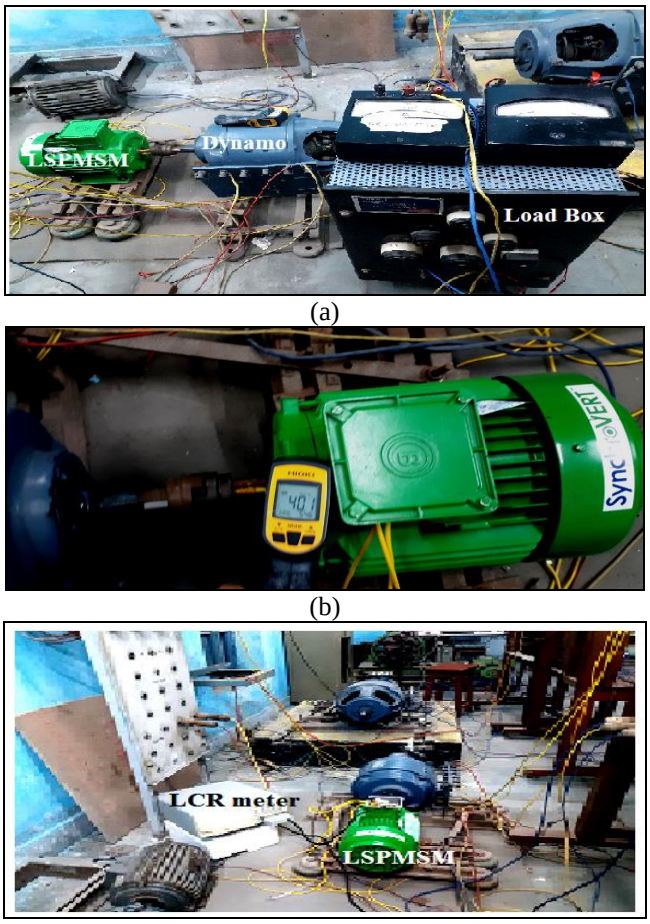

Figure 6. (a) Test set up of LSPMSM for temperature rise (b) Temperature of LSPMSM at driving end under full load condition (c) stator winding resistance measurement

A sharp increase in the temperature has been noticed in the test results. The stator winding temperature was calculated from measured winding resistance at motor terminals with the help of a LCR meter GW Instek LCR-816 immediately after the motor was turned off. The experimental set up for temperature measurement and stator winding resistances measurements have been displayed in Figure 6 (a), (b) and (c) respectively.

4. Results

In this section, results obtained at each step of the anticipated methodology have been validated with the test data.

4.1 Validation of Machine Dimension

The simulated model of the test motor has been developed in Ansys Maxwell environment. The core loss, copper loss and permanent magnet eddy current loss were estimated, as given in Table 2. The rotor total core loss has been segregated at three different parts: from shaft to lower part of PM, from PM to the outer periphery of rotor and the interpolar region of the rotor in a proportion to their volume.

Table 2 Losses in different parts of LSPMSM

Part of LSPMSM	Loss , W	Type of loss	Current source in LPTN
Shaft	14.43	Core loss	I_{10}
Rotor core 1	2.5	Core loss	I_9
Permanent Magnet	40.45	Eddy current loss	I_8
Rotor core 2 &3	0.03	Core loss	I_7
Rotor teeth	1.9	Core loss	I_6
Rotor bar	62.746	Ohmic loss	I_5
Stator teeth	1.85	Core loss	I_4
Stator conductor	225.6	Ohmic loss	I_3
Stator core	0.2	Core loss	I_2
Frame	0.0453	Core loss	I_1

4.2 Validation of Simulated Model with Actual Motor

Electromagnetic analysis has been conducted on the simulated model to obtain the performance at transients. The simulated results are shown in Figure 7. The output of the analysis shows that the motor steady state speed at full load is 1500 rpm which has been given in Figure 7 (a) while taking a per phase current of 2.24 A which has been shown in Figure 7 (b). Figure 7 (c) displayed the rated efficiency which is 89.2% at full load condition. This validates the results obtained from experiments.

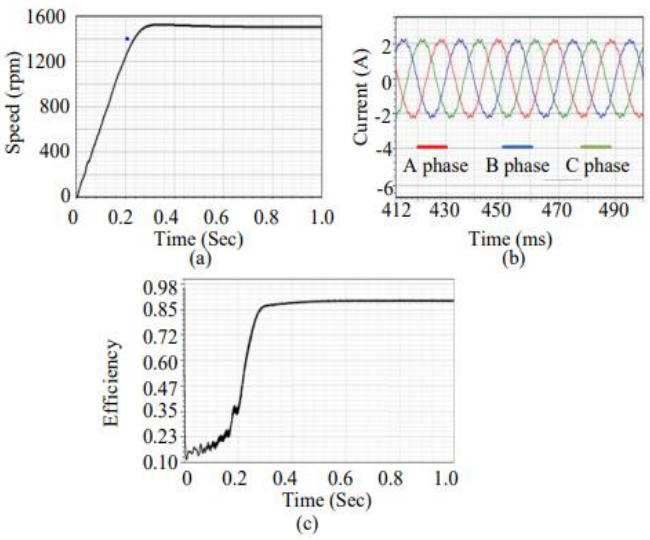

Figure 7. FEA results of (a) speed, (b) Line current and (c) efficiency of the tested machine.

4.3 Validation of Thermal Model

The motor has been tested under no load, half load and full load condition. In case of full load, the DE temperature rose exponentially from 30.2°C to 42.1°C in two hours constant run and when the motor stopped the temperature decreased exponentially from 42.1°C to the ambient whereas the NDE temperature increased exponentially from 30.2°C to 32.5°C and when the motor stopped the temperature rose sharply up to 34.8°C within 10 minutes and then started to decrease exponentially. Similarly, the DE temperature at half load condition rose from 30.3°C to 36.6°C and NDE temperature rose from 30.3°C to 32.2°C for continuous two hours run and sharp increase up to 33.4°C at NDE after the motor was stopped and then reduced exponentially. The same at no load are 31.4°C to 35.2°C at DE and 31.4°C to 32.3°C at NDE, then sharp increase up to 32.9°C. Physical test results and the simulated results for full, half and no load conditions at DE and NDE have been compared in Figure 8, 9 and 10 respectively.

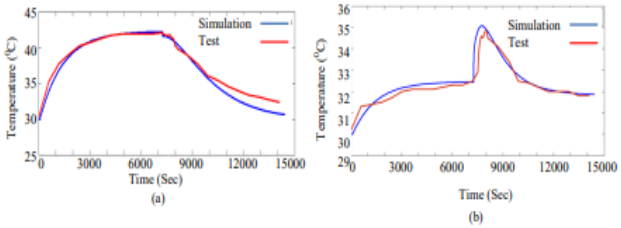

Figure 8. Simulated and physical test results for full load condition (a) at driving end (b) at non-driving end

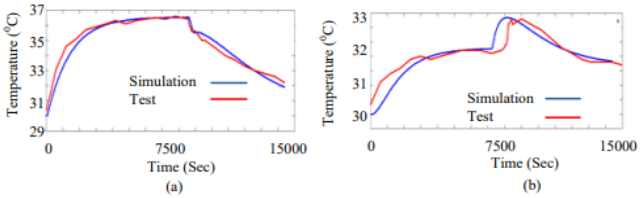

Figure 9. Simulated and physical test results for half load condition (a) at driving end (b) at non driving end

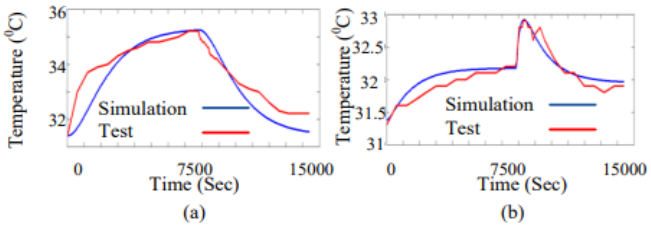

Figure 10. Simulated and physical test results for no load condition (a) at driving end (b) at non driving end

For the three predefined load conditions, the steady state temperatures for frame, stator, core, stator winding and permanent magnet of the LSPMSM have been presented in Table 3, which showed maximum temperature rise for PM was 84.27°C at full load condition.

Table 3. Steady state temperature at different part of LSPMSM for different load conditions

Part of LSPMSM	Temperature (°C)		
	Full load	Half load	No load
Stator winding	86.36	48.99	40.37
Frame	84.55	48.4	40.08
Stator core	84.96	48.53	40.15
Permanent magnet	84.27	55.62	49.31

At half load and no load conditions the permanent magnet losses being higher than the stator winding copper losses, the permanent magnet temperature was reached at highest level where as for full load condition stator winding has the highest temperature. Stator winding temperatures obtained from simulation and from the measurement of the resistance at different temperature by LCR meter have been compared in Figure 11.The winding resistance is temperature dependent and obeys the following relations:

$$R_T = R_0[1+\alpha(T_1 - T_0)] \quad (3)$$

$$or, T_1 = \frac{1}{\alpha}\left[\frac{R_T}{R_0} - 1\right] + T_0 \quad (4)$$

where, R_T and R_0 are the resistances at T_1 and T_0°C respectively,
and, α=3.9x10^{-3}Ω/°C is the temperature coefficient of copper.

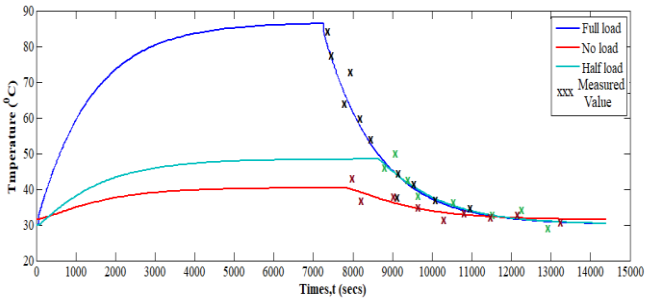

Figure 11. Simulated and measured temperature at stator winding

4.4 Modified Characteristics of LSPMSM

Due to the temperature rise reversible demagnetization takes place for permanent magnet N33UH. The revised coercivity and the remanence flux density have beeen plotted and hence its modified demagnetization characteristic has been shown by red line in Figure12.

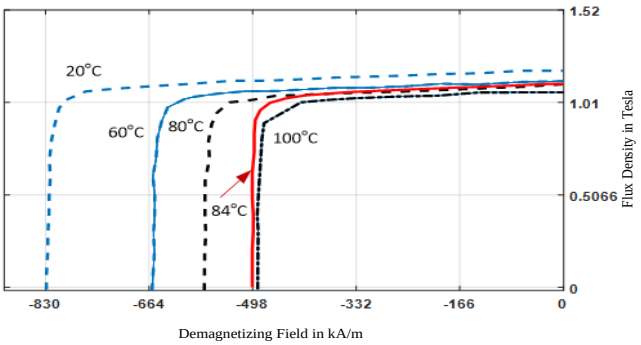

Figure 12. Modified demagnetizing characteristic of N33UH at 84.27°C

Magnetostatic analysis has been conducted on the developed model at full load to obtain the effect of demagnetization of PM on the performance of LSPMSM. The torque at steady state condition has been reduced, due to the reduction of the magnetic. Motor draws more power from the source resulting increased ohmic loss. The change in retentivity, coercivity, percentage change in torque and ohmic loss with temperature variation have been presented in Figure13 (a), (b), (c) and (d) respectively.

For the test motor the torque reduced by approximately 10.16 % and ohmic loss increased by about 6.5% as the temperature of PM has been increased to 84.27 °C which has been shown by red line in Figure13 (c) and (d) respectively.

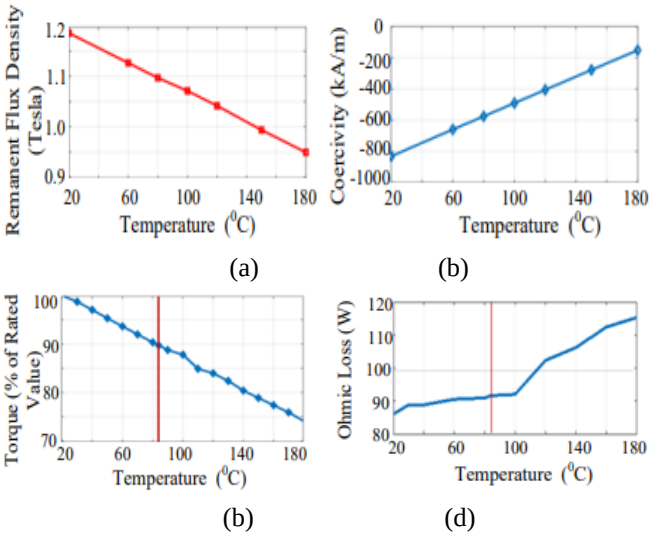

Figure 13. Effect of temperature variation in (a) Remanence flux density, (b) Coercivity, (c) Torque and (d) Ohmic loss of LSPMSM

5. Conclusion

The present work demonstrates that, demagnetization of the PMs caused due to the temperature rise at different load condition, has severe effect on the output performance of motor. The performance has degraded as the ohmic losses

have increased due to high temperature rise of the PM. This has led to reduction in torque developed in the said LSPMSM. Reduction of approximately 26.05 % in torque and about 34.05% increment in ohmic loss has been noticed in LSPMSM due to an overall temperature change for N33UH permanent magnet. Although for the test motor the variation in torque and ohmic loss is near about 10% at full load, in case of large rating machine performance degradation will consequently increase which could be analysed in further work. Hence, thermal analysis must be conducted to obtain the effect of temperature rise before selection of LSPMSM for particular application like EVs. The proposed soft tool is suitable for analyzing the performance in context of manufacturing LSPMSM, for particular application.

Authors' Contributions

Author-1 researched literature and did the modeling and simulation part.

Author-2 developed the physical system for validation of the software results

Author-3 carried out the overall analysis

Author-4 did the drafting of the paper subsequently all authors edited the whole paper so that the entire work is satisfactorily represented.

Conflict of interest: The authors do not have any conflict of interest

Funding source: This work is not supported by any type of funding agency.

Acknowledgements: The authors of this paper would like to convey their cordial thanks to the Department of Electrical Engineering, Jadavpur University, for providing all the assistances and also to allow conducting experiment in the laboratory. The authors are also grateful for the technical support provided by all the technical staffs of the department.

References

[1] J. G. Hayes, and G.A. Goodarzi, "Electric Power Train: Energy Systems, Power Electronics and Drives for Hybrid, Electric and Fuel Cell Vehicles", *First Edition*, John Wiley & Sons Limited, **2018**

[2] S. Rochi, "The Mars Mission – Technology for another world," Maxon Motors Application Stories, **2018**

[3] A.A. Adly& A. Huzayyin, "The Impact of Demagnetization on the Feasibility of Permanent Magnet Synchronous Motors in Industry Applications", *Journal of Advanced Research***17**, pp**103-108, 2019**

[4] S. K. Chowdhury and P. K. Baski, "A simple lumped parameter thermal model for electrical machine of TEFC design," *Joint International Conference on Power Electronics, Drives and Energy Systems & **2010** Power India*, New Delhi, India, pp.**1-7**, **2010.**

[5] Xu, Y, Xu, Z, Meng, Y, & Wang, Y. "Fluid-thermal characteristics of high-voltage line-start permanent magnet synchronous motor based on bidirectional hydraulic-thermal network coupling" *Engineering Science and Technology, an International Journal, **41**, Article **101386***.pp.**1-12,2023**

[6] Q. Chen, Z. Zou and B. Cao, "Lumped-parameter thermal network model and experimental research of interior pmsm for electric vehicle," in *CES Transactions on Electrical Machines and Systems*, vol. **1,** no. **4,** pp**. 367-374, 2017**.

[7] K. Bersch, S. Nuzzo, P.H. Connor, C.N. Eastwick, M. Galea, R. Rolston and G. Vakil "Combined Thermo fluid and Electromagnetic Optimization of Stator Vent Cooling," *XIII International Conference on Electrical Machines (ICEM)*,

[8] A. Tikadar, N. Kumar, Y. Joshi and S. Kumar, "Coupled Electro-Thermal Analysis of Permanent Magnet Synchronous Motor for Electric Vehicles,"*19th IEEE Intersociety Conference on Thermal and Thermo mechanical Phenomena in Electronic Systems (ITherm)*, Orlando, FL, USA, **2020**

[9] A. Tikadar, J. W. Kim, Y. Joshi and S. Kumar, "Flow-Assisted Evaporative Cooling for Electric Motor," *IEEE Transactions on Transportation Electrification*, vol. **8**, no. 1, pp. 1128-1143, March 2022

[10] A. L. Rodríguez, P. Lombard, V. Leconte, P. Wendling and I. Villar, "Thermal modelling of a Permanent Magnet Synchronous Machine through FEM simulation with experimental validation," *2020 IEEE*

[11] M. Cheng, S. Ding, W. Li, P. Zhang, Q. Wang and M. Duan, "Cooling System Design and Thermal analysis of a PMSM for Rail Transit," *2020 15th IEEE Conference on Industrial Electronics and Applications (ICIEA)*, Kristiansand, Norway, 2020, pp. 1912-1915

[12] Q. Chen, Z. Zou and B. Cao, "Lumped-parameter thermal network model and experimental research of interior pmsm for electric vehicle," in *CES Transactions on Electrical Machines and Systems*, Vol.**1**, no.**4**, pp. **367-374**, **2017**.

[13] Liang, Dawei& Zhu, Z.Q. & Zhang, Yafeng & Feng, Jianghua & Guo, Shuying& Li, Yifeng & Wu, Jiangquan& Zhao, Anfeng "A Hybrid Lumped-Parameter and 2-D Analytical Thermal Model for Electrical Machines" *IEEE Transactions on Industry Applications.* pp. **1-1**.

[14] S. Mukundan, H. Dhulipati, J. Tjong and N. C. Kar, "Parameter Determination of PMSM using Coupled Electromagnetic and Thermal Model Incorporating Current Harmonics," *2018 IEEE International Magnetics Conference (INTERMAG)*, Singapore, **2018**, pp. **1-1**.

[15] C. Liu, J. Zou, Y. Xu and G. Yu, "An Efficient Thermal Computation Model of PMSM Based on FEA Results and Interpolation," in *IEEE Transactions on Applied Superconductivity*, vol. **31**, no. **8**, pp. **1-4,** Nov. **2021**.

[16] Y. Ryu, S. W. Hwang, J. W. Chin, Y. S. Hwang, S. W. Yoon and M. -S. Lim, "Mathematical Modeling of Fast and Accurate Coupled Electromagnetic-Thermal Analysis," in *IEEE Transactions on Industry Applications*, vol. **57**, no. **5**, pp. **4636-4645**, Sept.-Oct. **2021**.

[17] D. Liang *et al*., "Estimation of Two- and Three-Dimensional Spatial Magnet Temperature Distributions for Interior PMSMs Based on Hybrid Analytical and Lumped-Parameter Thermal Model," *IEEE Transactions on Energy Conversion*, vol. **37**, no. **3**, pp. **2175-2189**, Sept. **2022**.

[18] C. Debruyne, M. Polikarpova, S. Derammelaere, P. Sergeant, J Pyrhönen, J.J.M. Desmet, L. Vandevelde, "Evaluation of the Efficiency of Line-Start Permanent-Magnet Machines as a Function of the Operating Temperature", *IEEE Transactions on Industrial Electronics*, Vol. **61**, No. **8**, pp. **4443-4454, 2014**.

[19] P. Bhattacharya, A. Roy, "Condition Monitoring System of a Three Phase Induction Motor Against Thermal Overloading" *International Journal of Computer Sciences and Engineering*, Vol.**07**, Special Issue.**18**, pp**.305-308, 2019.**

[20] Anurag Singh Tomer and S.P.Dubey , "Response Based Tunning of Proportional and Integral Constants in PI Controlled Six Phase PMSM Drive*", International Journal of Computer Sciences and Engineering*, Vol.**3,** Issue.**12**, pp.**23-28, 2015**.

[21] M. F. Palangar, A. Mahmoudi, S. Kahourzade and W. L. Soong, "Electromagnetic and Thermal Analysis of a Line-Start Permanent-Magnet Synchronous Motor," *2020 IEEE Energy Conversion Congress and Exposition (ECCE)*, Detroit, MI, USA, pp**.502-508**, **2020.**

[22] F. J. T. E. Ferreira, B. Leprettre, A. Q. Duarte and A. T. De Almeida, "Comparison of protection requirements in IE2-, IE3-, and IE4-class motors," *IEEE International Electric Machines &*

Drives Conference (IEMDC), Coeur d'Alene, ID, USA, pp.**1874-1880, 2015.**

[23] Putek, P., Pulch, R., Bartel, A. *et al.* Shape and topology optimization of a permanent-magnet machine under uncertainties. *J.Math.Industry* **6, 11, 2016.**

[24] M. J. Bala, N. K. Deb and S. K. Chowdhury, "Improvement of the performances of line start permanent magnet synchronous motor with flux barrier in the rotor," *2017 IEEE Calcutta Conference (CALCON)*, pp. **357-361, 2017.**

[25] J.F. Gieras, "Permanent Magnet Motor Technology: Design and applications", *Third Edition*, CRC Press, Taylor & Francis Group, **2010,**ISBN 978-1-4200-6440-7.

[26] L. Uršič & M. Nemec,"Permanent Magnet Synchronous Machine Demagnetization Prevention and Torque Estimation Control Considering Rotor Temperature" *IET Power Electronics*, 2019, **12.10.1049**/iet-pel.**2018.6162.**

[27] F. Qi, M. Schenk, R. W. De Doncker, "Discussing details of lumped parameter thermal modelling in electrical machines,'' 7th *IET International Conference on Power Electronics, Machines and Drives(PEMD 2014)*, Manchester, UK, pp.**1-6, 2014.**

[28] A. Kačenka, A. -C. Pop, I. Vintiloiu and D. Fodorean, "Lumped Parameter Thermal Modeling of Permanent Magnet Synchronous Motor," *2019 Electric Vehicles International Conference (EV)*, Bucharest, Romania, pp**.1-6**, **2019.**

[29] David A. Staton and Andrea Cavagnino "Convection Heat Transfer and Flow Calculations Suitable for Electric Machines Thermal Models" *IEEE transactions on Industrial Electronics*, Vol.**55**, no**. 10**, **2008**.

[30] Ogbonnaya I. Okoro, ''Steady and Transient States Thermal Analysis of a 7.5-kW Squirrel-Cage Induction Machine at Rated-Load Operation'', *IEEE Transactions on Energy Conversion*, vol. **20**, no. **4**, December **2005**, pp.**730, 2005.**

[31] P. R .Mellor, D. .Roberts and D. R. Turner, "Lumped parameter thermal model for electrical machines of TEFC design", *IEE Proc.B*, vol.**138**, no.**5**, September, pp. **205, 1991**.

[32] M. J. Bala, C. Jana, S. K. Chowdhury and N. K. Deb, "Performance analysis of different rotor configuration of LSPMSM for Electric Vehicles," *2022 IEEE Calcutta Conference (CALCON)*, Kolkata, India, pp. **223-227, 2022.**

AUTHORS' PROFILE

Mousumi Jana Bala received her Bachelor Degree in Electrical Engineering from Bengal Engineering College, Shibpur (Now IIEST), West Bengal, India in 2002 and Master Degree in Electrical Engineering from Jadavpur University, West Bengal, India in 2008. She is now working as an Assistant Professor in the Department of Electrical Engineering in Meghnad Saha Institute of Technology, Kolkata, India since 2018. She is working on design of Electrical Machines in the Department of Electrical Engineering, Jadavpur University, India for Ph.D. thesis.

Chandan Jana received his Bachelor Degree and Master degree in Electrical Engineering from Jadavpur University, Kolkata, India in 1998 and 2001 respectively. Now, he is working as Assistant Professor in the Department of Electrical Engineering in Hooghly Engineering and Technology College, Chinsurah, West Bengal, India. He has a teaching experience of 22 years. He is now working for Ph.D. thesis on Power System Disturbances in the Department of Electrical Engineering, Jadavpur University, India. His current research interest includes Machine Learning, Distributed Generation, and Electrical Machine Design.

Dr. Suparna Kar Chowdhury graduated in Electrical Engineering from Jadavpur University, Kolkata, India in the year of 1987. She received her Master of Technology degree in Electrical Engineering from IIT, Kharagpur, India in 1989. She is serving as an Assistant Professor in Jadavpur University, India in since 1990. She was awarded with PhD. in Electrical Engineering in 2000 from Jadavpur University. Currently she is working as a Professor in Electrical Engineering Department, Jadavpur University. Her interest of work includes design of electrical machine and analysis.

Dr. Arindam Kumar Sil received his Bachelor Degree in Electrical and Electronics Engineering from Karnataka University, Dharwad, India. He received his Master Degree in Power Engineering from Jadavpur University, India. He was awarded his PhD degree in Electrical Engineering from Jadavpur University, India. He is currently working as an Associate Professor at the Department of Electrical Engineering, Jadavpur University, India. His recent research interests include working into Planning of Power System, Renewable Energy Integration to Grid and Peak Load Management.

